PRAMANA
— journal of
physics

Vol. 77, No. 5
November 2011
pp. 929–947

Solitons in Bose–Einstein condensates

RADHA BALAKRISHNAN[1,*] and INDUBALA I SATIJA[2,3]

[1]The Institute of Mathematical Sciences, Chennai 600113, India
[2]Department of Physics, George Mason University, Fairfax, VA 22030, USA
[3]National Institute of Standards and Technology, Gaithersburg, MD 20899, USA
*Corresponding author. E-mail: radha@imsc.res.in

Abstract. The Gross–Pitaevskii equation (GPE) describing the evolution of the Bose–Einstein condensate (BEC) order parameter for weakly interacting bosons supports dark solitons for repulsive interactions and bright solitons for attractive interactions. After a brief introduction to BEC and a general review of GPE solitons, we present our results on solitons that arise in the BEC of hard-core bosons, which is a system with strongly repulsive interactions. For a given background density, this system is found to support both a dark soliton and an antidark soliton (i.e., a bright soliton on a pedestal) for the density profile. When the background has more (less) holes than particles, the dark (antidark) soliton solution dies down as its velocity approaches the sound velocity of the system, while the antidark (dark) soliton persists all the way up to the sound velocity. This persistence is in contrast to the behaviour of the GPE dark soliton, which dies down at the Bogoliubov sound velocity. The energy–momentum dispersion relation for the solitons is shown to be similar to the exact quantum low-lying excitation spectrum found by Lieb for bosons with a delta-function interaction.

Keywords. Solitons; Bose–Einstein condensates; hard-core bosons; spin Hamiltonians.

PACS Nos 03.75.Lm; 03.75.Kk; 05.45.Yv; 75.10.Pq

1. Introduction

A certain class of nonlinear evolution equations can support solitary wave/soliton solutions [1]. A solitary wave is a localized travelling wave solution that does not spread or disperse, but retains its size, shape and speed when it moves. It arises provided the nonlinearity is such that the defocussing effect of the dispersive term and the steepening effect of the nonlinear terms in the equation balance each other, so as to give a localized profile for the solution. If after a collision of two solitary waves, each wave comes away unscathed, with its size, shape and speed intact, such a solitary wave is called a soliton. Thus a soliton is a solitary wave with a special collision property. However, it is to be noted that in physics literature, a solitary wave is customarily referred to as a soliton, due to its particle-like behaviour during propagation. We shall also do so in this article. Solitons arise in a variety of fields such as hydrodynamics, plasma physics, signal propagation in optical fibres, magnetism, etc. [2].

DOI: 10.1007/s12043-011-0187-z; ***e*Publication: 31 October 2011**

After the experimental realization of a Bose–Einstein condensate (BEC) [3] in a trapped ultracold Bose gas of alkali atoms (such as Rb, Na and Li), the study of solitons in this intrinsically nonlinear system has become a topic of current interest, both experimentally [4–6] and theoretically [7–9]. A BEC is characterized by the macroscopic occupation of bosons in a single quantum level, usually the ground state. This condensed state is a 'matter wave' analogous to a laser where all atoms in the condensate are phase coherent. Thus, widely spaced atoms can have an interference pattern, with quantum effects manifested on a macroscopic scale. The nonlinear effects in a BEC depend crucially on the type of interaction between the bosons.

In this paper, we study soliton propagation in the BEC of a hard-core boson (HCB) system, which is a system of bosons with strongly repulsive interactions [10]. The paper is organized as follows. Starting with the Hamiltonian operator for an interacting boson system, the concept of a broken gauge symmetry in a BEC is introduced in §2. In §3, the well-known Gross–Pitaevskii equation (GPE) for the BEC order parameter in a weakly interacting boson system is presented and its linear excitations are discussed. In §4, nonlinear excitations of the GPE are reviewed, including dark solitons for bosons with weakly repulsive interactions, and bright solitons for weakly attractive interactions. The nonlinear evolution equation for the BEC order parameter of the HCB condensate is derived in §5. Linear excitations and nonlinear excitations, i.e., dark solitons and antidark solitons (i.e., bright solitons on a pedestal [11]) supported by this equation are found in §6. Section 7 discusses the various novel features of these HCB solitons, including the emergence of persistence solitons. Energy–momentum dispersion relation for the solitons is determined in §8. A summary of our results is given in §9.

2. Interacting Bose system

The many-body Hamiltonian for a system of interacting bosons is given by

$$H = -\int \Psi^\dagger \left[\frac{\hbar^2}{2m}\nabla^2 + \mu\right]\Psi \mathrm{d}\mathbf{r} + \frac{1}{2}\int \Psi^\dagger(\mathbf{r})\Psi^\dagger(\mathbf{r}')V(\mathbf{r}'-\mathbf{r})\Psi(\mathbf{r})\Psi(\mathbf{r}')\mathrm{d}\mathbf{r}'\mathrm{d}\mathbf{r}, \tag{1}$$

where Ψ is the boson field operator satisfying the commutation relation $[\Psi(\mathbf{r}), \Psi^\dagger\mathbf{r}'] = \delta(\mathbf{r} - \mathbf{r}')$, $V(\mathbf{r}' - \mathbf{r})$ is the two-body interaction and μ is the chemical potential. The dynamics is found to be

$$i\hbar\frac{\partial\Psi}{\partial t} = [\Psi, H] = \left[-\frac{\hbar^2}{2m}\nabla^2 + \int \Psi^\dagger(\mathbf{r}')V(\mathbf{r}' - \mathbf{r})\Psi(\mathbf{r}')\mathrm{d}\mathbf{r}' - \mu\right]\Psi(\mathbf{r}). \tag{2}$$

2.1 *Broken gauge symmetry*

The invariance of H under a global $U(1)$ gauge transformation $\Psi \rightarrow \Psi\exp(i\phi)$ suggests the following analogy with respect to the concept of a broken rotational symmetry in an isotropic Heisenberg ferromagnetic Hamiltonian $H_{\mathrm{FM}} = \sum_{\langle ij\rangle} J_{ij}\mathbf{S}_i \cdot \mathbf{S}_j$. This spin Hamiltonian is invariant under simultaneous rotation of all spins. But below the Curie temperature, $\langle\mathbf{S}\rangle \neq 0$, and the direction of magnetization is well defined. In analogy with

the above, BEC order parameter (also called the condensate wave function) for the Bose system is defined as $\psi = \langle\Psi\rangle$, the expectation value of the Bose operator. For $T > T_c$, where T_c is the Bose–Einstein condensation temperature, the bosons are normal so that $\langle\Psi\rangle$ vanishes. But below T_c, $\langle\Psi\rangle \neq 0$ (in analogy with the spin system), and a corresponding definite phase of the BEC order parameter gets selected.

Further, for $T < T_c$, since the order parameter (or condensate wave function) is $\langle\Psi\rangle$, the condensate density is given by $\rho^s = \langle\Psi^\dagger\rangle\langle\Psi\rangle$. On the other hand, the total density $\rho = \langle\Psi^\dagger\Psi\rangle$. Hence for a general interacting system, $(\rho - \rho^s)$ is nonzero implying the presence of quantum fluctuations and depletion.

3. Weakly interacting Bosons: Gross–Pitaevskii equation (GPE) for the condensate order parameter

Consider a dilute gas whose range of interatomic forces r_0 is much greater than the average distance between atoms $d = n^{-1/3}$, where n is the density. For large d, the asymptotic expression for the wave function, which depends on the scattering amplitude, can be used. For $T < T_c$, since relevant momenta are small, the scattering amplitude becomes independent of energy, and is replaced by its low-energy value, determined by the s-wave scattering length $\bar{a}$. An effective soft potential V_{eff} which has the same low-energy scattering properties as $V(\mathbf{r} - \mathbf{r}')$ is introduced. It is defined using $g = \int V_{\text{eff}}(\mathbf{r})\,\mathrm{d}\mathbf{r} = 4\pi\hbar^2\bar{a}/m$, where m is the atomic mass. In effect, $V(\mathbf{r} - \mathbf{r}')$ can be replaced by a contact potential $g\delta(\mathbf{r} - \mathbf{r}')$ in the dynamical eq. (2). After making the transformation $\Psi \to \Psi \exp(i\mu t/\hbar)$ and by just replacing the operator Ψ by its expectation value $\psi = \langle\Psi\rangle$, the following Gross–Pitaevskii equation (GPE) is obtained for the time evolution of the condensate order parameter ψ, in the case of weakly interacting bosons:

$$i\hbar\frac{\partial\psi}{\partial t} + \frac{\hbar^2}{2m}\nabla^2\psi - g|\psi|^2\psi = 0. \tag{3}$$

This is a nonlinear partial differential equation, with the interaction term g giving rise to the nonlinearity. Note that $\bar{a} > 0$ $(g > 0)$ implies a repulsive interaction, while $\bar{a} < 0$ $(g < 0)$ implies an attractive interaction.

As is obvious in this case, $\rho = \langle\Psi^\dagger\Psi\rangle = \psi^*\psi = \rho^s$. Thus the total density is equal to the condensate density, and hence both quantum fluctuations and depletion are absent in GPE dynamics.

Although GPE has an underlying quantum nature, the condensate order parameter has a macroscopic extent, suggesting observation of quantum effects on a macroscopic, classical scale.

3.1 *Linear excitations in GPE*

At very low temperatures, the energy–momentum dispersion relation for the small amplitude excitations can be found from the frequencies of the linearized GPE with plane-wave solutions. Small deviations around the background density ρ_0 are studied by setting $\psi(\mathbf{r}, t) = \sqrt{\rho_0} + \delta\psi$, in eq. (3), with

$$\delta\psi = A\,\exp\,(i(\mathbf{k}\cdot\mathbf{r} - \omega t)) + B\,\exp(-i(\mathbf{k}\cdot\mathbf{r} - \omega t)). \tag{4}$$

The dispersion relation is found to be

$$\omega^2(k) = \frac{\rho_0\, g}{m}k^2 + \frac{\hbar^2 k^4}{4m^2}. \tag{5}$$

Two cases arise:

(i) *Repulsive interaction* ($g > 0$)
This leads to the following Bogoliubov spectrum:

$$\omega(k) = \sqrt{c^2k^2 + \frac{\hbar^2 k^4}{4m^2}}, \tag{6}$$

where

$$c = \sqrt{\rho_0\, g/m} \tag{7}$$

is called the Bogoliubov sound velocity. This is because for small momenta, the excitations are phonon-like, with $\omega = ck$, linear in k. For large k, $\omega = \hbar^2k^2/2m$, quadratic in k. These excitations are dynamically stable for all k, since $\omega^2 \geq 0$.

(ii) *Attractive interaction* ($g < 0$)
In this case, there is dynamical stability only if

$$-\frac{\rho_0\,|g|}{m}k^2 + \frac{\hbar^2 k^4}{4m^2} \geq 0.$$

On substituting for g, this leads to the condition $k^2 \geq 16\pi\rho_0\bar{a}$ for stability. In other words, there is no associated sound velocity such as eq. (7) for the attractive case. For a particle in a box of length L, the lowest nonzero momentum is $2\pi/L$, which leads to the condition $N|\bar{a}|/L \leq (\pi/4)$.

3.2 *Magnetic traps: From 3D to 1D GPE*

Trapping of a BEC takes advantage of the magnetic interaction energy $-\boldsymbol{\mu}\cdot\mathbf{B}$, where $\boldsymbol{\mu}$ is the magnetic moment of the alkali atom and $\mathbf{B}$ is the magnetic field. For experiments with Rb and Na, the confining potential due to the magnetic trap can be approximated with a quadratic form: $V(\mathbf{r}) = \frac{1}{2}m\Omega^2[(y^2+z^2)+\lambda x^2]$. For $\lambda \ll 1$, this gives a cigar-shaped trapped cloud. By writing the condensate wave function as $\psi(\mathbf{r}) = \sqrt{N/l^3}\,F(R)\chi(s,\alpha_0)$, where $l = \sqrt{\hbar/m\Omega}$, $R = \sqrt{(y^2+z^2)}/l$, $s = x/l$ and $\alpha_0 = \Omega t$, a rigorous derivation of Lieb *et al* [12] shows that a GPE for $\chi(s,\alpha_0)$ can be obtained as the 1D limit of the 3D mean-field theory, rather than a 1D mean-field theory.

4. Nonlinear excitations of the GPE

In this section, we review the known exact results for soliton solutions of the GPE (eq. (3)), for the condensate of bosons with weak repulsive interaction ($g > 0$) and weak attractive interaction ($g < 0$), by studying unidirectional dynamics in quasi-one-dimensional traps.

4.1 *Repulsive interaction ($g > 0$): Dark solitons*

By looking for unidirectional travelling wave solutions of eq. (3) of the form $\psi(z) = \sqrt{\rho(z)}\exp(i\phi(z))$, where $z = (x - vt)/\xi$ is a dimensionless variable, we get $\xi = \hbar/\sqrt{2mg\rho_0}$. Here ξ is the healing length and ρ_0 is the background density. (ξ turns out to be the typical length scale of interaction obtained by equating kinetic and potential energies, i.e., $(p^2/2m) = (\hbar/\xi)^2/2m = g\rho_0$.)

Imposing the boundary conditions $|\psi(z)|^2 \to \rho_0$ and $\mathrm{d}\psi/\mathrm{d}z \to 0$, as $z \to \pm\infty$, one obtains

$$\psi(z) = \sqrt{\rho_0}\ \left(\gamma\ \tanh\frac{\gamma z}{\sqrt{2}} + i\frac{v}{c}\right) = \sqrt{\rho(z)}\exp(i\phi(z)). \tag{8}$$

Here, $\gamma = \sqrt{\left(1 - \frac{v^2}{c^2}\right)}$, where $c = \sqrt{g\rho_0/m}$ is the Bogoliubov sound velocity that appeared in eq. (7).

The solution (8) shows that both the density profile $\rho(z)$ and the phase profile $\phi(z)$ travel with the same speed v.

For $v \le c$, γ is real, and the condensate wave function $\psi(z)$ takes on different constant complex values as $z \to \pm\infty$. However, when $v = 0$, the complex order parameter ψ becomes a real kink solution with asymptotic values $\pm\sqrt{\rho_0}$ as z goes to $\pm\infty$.

In general, eq. (8) corresponds to the following density profile:

$$\rho(z) = |\psi(z)|^2 = \rho_0\left[1 - \gamma^2\ \mathrm{sech}^2\left[\frac{\gamma z}{\sqrt{2}}\right]\right]. \tag{9}$$

For $v \le c$, $\rho(z) \to \rho_0$ as $z \to \pm\infty$. There is a suppression of density (i.e., absence of atoms) at the centre of the BEC soliton, with respect to the background value ρ_0, for all $0 < v < c$.

As $v \to 0$, $\rho(z)$ dips to zero at the soliton centre.This is called a dark soliton.

As v increases, the width of the soliton increases. $\rho(z)$ dips to a non-zero value $\rho_0[1-\gamma^2]$ at the centre. This is sometimes called a gray soliton.

As $v \to c$, $\rho(z) \to \rho_0$ for all z. Thus the dark soliton flattens out and disappears as $v \to c$.

Phase jump of GPE soliton

From eq. (8), we see that as z varies from $-\infty$ to ∞, the phase of the condensate wave function jumps by

$$\Delta\phi = 2\cos^{-1}(v/c). \tag{10}$$

Thus the static soliton with $v = 0$ is a kink solution which is real, and has the maximum phase jump of π across the centre of the soliton.

4.2 *Attractive interaction ($g < 0$): Bright solitons*

Unidirectional travelling wave solutions of eq. (3) with $g = -|g|$ have the following form:

$$\psi = A_0\ \mathrm{sech}\left[\sqrt{\frac{|g|}{2}}(x - u_d t)A_0\right]\exp\left[iu_d(x - u_p t)/2\right]. \tag{11}$$

In (11), u_d and u_p are the speeds of the density profile and phase profile, respectively. which can be positive or negative and $A_0 = \sqrt{u_d(u_d - 2u_p)/2|g|}$.

This leads to the density profile

$$\rho(z) = A_0^2 \operatorname{sech}^2\left[\sqrt{\frac{|g|}{2}}(x - u_d t)A_0\right]. \tag{12}$$

For real A_0, this leads to the vanishing of $\rho(z)$ as z goes to $\pm\infty$, with maximum density at the soliton centre. Hence eq. (12) represents a bright soliton, with the background density zero.

Note that for A_0 to be real, the condition $u_d(u_d - 2u_p) > 0$ must be satisfied, implying that $u_d \neq u_p$. Thus the density and phase of the bright soliton of the attractive GPE always travel with different speeds, contrary to the solitons of the repulsive GPE, where they travel with the same speed. The bright soliton flattens out for $u_d = 0$, for all u_p, since its amplitude A_0 vanishes. Thus the static bright soliton profile is flat, unlike the static dark soliton profile.

As an example, for $u_p = 0$, the amplitude of the bright soliton increases as u_d increases. On the other hand, the amplitude of the soliton of the repulsive GPE decreases as its speed increases, flattening out at the Bogoliubov sound velocity.

Finally, contrary to the repulsive GPE case, the phase profile of the soliton of the attractive GPE does not have a phase jump across the soliton centre, since it is a linear function of $(x - u_p t)$, as seen from (11).

4.3 *Experiments*

Using a cigar-shaped trap, phase-imprinting method has been used to create and study dark solitons in an ultracold gas of ^{87}Rb atoms with weakly repulsive interaction, i.e., positive scattering length [4]. Dark solitons have also been observed in a dilute gas of ^{23}Na atoms [5]. Tuning the scattering length $\bar{a}$ from positive to negative values has become possible using Feschbach resonances by varying the magnetic field. Bright solitons have been created in ^{7}Li [6] for small negative values of $\bar{a}$.

5. Hard-core bosons: Nonlinear evolution equation for the condensate order parameter

In the last section, we saw that the condensate order parameter for a weakly interacting system satisfies the GPE and supports solitons. In particular, we have seen that the weakly repulsive (or soft-core) Bose condensate supports dark solitons. This motivates us to ask: What is the evolution equation for the condensate order parameter in a strongly repulsive Bose condensate? Does it support solitons, and if so are they similar to the GPE solitons? To answer these, we study a system of hard-core bosons, which is an example of a strongly repulsive system.

It is interesting to study the dynamics of the condensate of a hard-core boson system theoretically because firstly, it has become possible to create optical lattices in the laboratory using standing waves of laser light, load BEC atoms on such lattices, and also tune the interactions between atoms. It is therefore possible to simulate a hard-core system with

not more than one boson per lattice site, and also study the dynamics of its BEC experimentally. Secondly, the exact low-energy dispersion relation for quantum excitations in a Bose gas on a line, with delta-function interactions (including the HCB limit) has been studied by Lieb [13]. It is therefore important to theoretically study dynamical excitations (both linear and nonlinear) of a condensate of hard-core bosons in a quasi-one-dimensional scenario and analyse their behaviour.

5.1 *The Bose–Hubbard model for hard-core bosons with nearest-neighbour interactions*

We begin with the following Hamiltonian for the extended Bose–Hubbard model [14] describing bosons hopping on a d-dimensional lattice:

$$H = -\sum_{j,a}\left[t\, b_j^\dagger b_{j+a} + V n_j n_{j+a}\right] + \sum_j U n_j(n_j - 1) - (\mu - 2t)n_j. \tag{13}$$

Here, $b_j^\dagger$ (b_j) are boson creation (annihilation) operators at lattice site j, satisfying the commutation relation $\left[b_i, b_j^\dagger\right] = \delta_{ij}$, $n_j = b_j^\dagger b_j$ is the number operator, a labels nearest-neighbour (NN) sites, t is the NN hopping parameter, and $U \gg 0$ is a strong, on-site repulsive interaction. An attractive NN interaction $-V$ (with $V > 0$) has been introduced to soften the strong repulsion. μ is the chemical potential. We have added the on-site term $2tn_j$ so that in the continuum description, (13) leads to the correct form for the kinetic energy term in the many-body bosonic Hamiltonian (1), with the identification $t = \hbar^2/ma^2$.

In the Hamiltonian (13), the limit $U \to \infty$ implies that an infinite energy is needed to place two bosons at the same site. Such bosons are hard-core bosons (HCB), i.e., bosons with the (fermion-like) constraint that two bosons cannot occupy the same site. Thus HCB creation and annihilation operators anticommute at the same site but commute at different sites. That is, $b_j^2 = 0$; $n_j^2 = n_j$; $\left\{b_j, b_j^\dagger\right\} = 1$, and $\left[b_j, b_l^\dagger\right] = 0$ for $j \neq l$. Combining these relations, we see that the HCB creation and annihilation operators must satisfy

$$\left[b_j, b_l^\dagger\right] = (1 - 2n_j)\delta_{jl}. \tag{14}$$

Identifying

$$b_j = S_j^+; \quad n_j = \frac{1}{2} - S_j^z, \tag{15}$$

where $S_j^+ = \left(S_j^x + i S_j^y\right)$ and S_j^z represent the spin-raising operator and the operator for the z component, respectively, we see that HCB algebra (14) can be identified [15] with the algebra $\left[S_j^+, S_l^-\right] = 2S_j^z\,\delta_{jl}$ for a quantum spin with $S = \frac{1}{2}$.

Using the identification (15), the Bose–Hubbard Hamiltonian (13) for the HCB case becomes the following XXZ quantum spin Hamiltonian in a magnetic field:

$$H_S = -\sum_{j,a}\left[t S_j^+ S_{j+a}^- + V S_j^z S_{j+a}^z\right] - [(t - V)d - \mu]\sum_j S_j^z. \tag{16}$$

The magnetic field along the z-direction is $\left((t - V)d - \mu\right)$.

The dynamics of the HCB system (16) is described by the Heisenberg equation of motion for the spin-raising operator S_j^+,

$$i\hbar \frac{\partial S_j^+}{\partial \tau} = \left[S_j^+, H_S\right] = [(t-V)d - \mu]S_j^+ - tS_j^z \sum_a S_{j+a}^+ + VS_j^+ \sum_a S_{j+a}^z, \tag{17}$$

where τ stands for time.

5.2 *Spin-coherent state formulation*

With the identification (15) of the HCB operators with spin operators, the BEC order parameter of the HCB system is given by $\eta_j = \langle b_j \rangle = \langle S_j^+ \rangle$. The inherent coherence in the condensed phase of the hard-core boson system suggests that the natural choice of state [16] to compute the above expectation value of the spin-raising operator is the spin-coherent state [17]. This choice is analogous to the use of boson coherent states to describe the condensate of a regular boson system with weak interactions, which leads to the GPE for the order parameter [18]. Coherent states are most useful in the context of many-body systems which behave classically. Coherent state representation has been used to describe the order parameter in the superfluid He^4.

The spin-S coherent state [17] at a lattice site j is defined by $|\mu_j\rangle = (1 + |\mu_j|^2)\exp[\mu_j S_j^-]|0\rangle$, where $S_j^- = S_j^x - iS_j^y$ is the spin-lowering operator and μ_j is a complex quantity. $S_j^z|S\rangle = S|0\rangle$. For N spins, we work with the direct product $|\mu_N\rangle = \Pi_j^N |\mu_j\rangle$. The states $|\mu_j\rangle$ are normalized, nonorthogonal and overcomplete. It is convenient to use the parametrization: $\mu_j = \tan(\theta_j/2)\exp(i\phi_j)$, where $0 \le \theta_j \le \pi$ and $0 \le \phi_j \le 2\pi$. This parametrization has the advantage that the diagonal matrix elements of single spin operators in the spin-coherent representation become identical to the corresponding expressions for a classical spin vector $\mathbf{S}_j = S(\sin\theta_j \cos\phi_j,\ \sin\theta_j \sin\phi_j,\ \cos\theta_j)$, with polar angle θ_j and azimuthal angle ϕ_j. However, not surprisingly, this correspondence between quantum expectation values and classical spin values does not carry over to products of operators. As an example, we can show that $\langle S_j^- S_j^+ \rangle$ is not equal to the classical value $S^2 \sin^2\theta_j$ (see the paragraph below eq. (18)).

Since $S = \frac{1}{2}$ for our system, we have $|\mu_j\rangle = \cos(\theta_j/2)|\uparrow\rangle + \exp i\phi_j \sin(\theta_j/2)|\downarrow\rangle$, where $|\uparrow\rangle$ and $|\downarrow\rangle$ represent spin-up and spin-down states, respectively. In this case, by taking the spin-coherent state averages, we obtain the following expressions for the various physical quantities of interest. The condensate order parameter is

$$\eta_j = \langle S_j^+ \rangle = \frac{1}{2}\sin\theta_j \exp(i\phi_j) = \sqrt{\rho_j^s}\exp(i\phi_j). \tag{18}$$

Hence the condensate number density $\rho_j^s = |\eta_j|^2 = \frac{1}{4}\sin^2\theta_j$. The particle number density $\rho_j = \langle n_j \rangle = \langle S_j^- S_j^+ \rangle = \left\langle \left((S_j^x)^2 + (S_j^y)^2 + i[S_j^x, S_j^y]\right)\right\rangle = \left\langle \left(S^2 - S_j^{z2} - S_j^z\right)\right\rangle == \langle(\frac{1}{2} - S_j^z)\rangle = \sin^2(\theta_j/2)$ where we have used the spin-coherent state average $\langle S_j^z \rangle = \cos\theta_j$. This leads to the relationship

$$\rho_j^s = \rho_j(1 - \rho_j). \tag{19}$$

Hence, contrary to GPE case discussed in §3, $\rho_j^s \neq \rho_j$. This implies the presence of depletion in the HCB system.

Further, substituting (19) in (18), we obtain

$$\eta_j = \sqrt{\rho_j(1-\rho_j)}\,\exp(i\phi_j). \tag{20}$$

The presence of quantum fluctuations can be seen from relations such as $\langle S_j^- S_j^+\rangle - \langle S_j^-\rangle\langle S_j^+\rangle = \rho_j^2$ and $\langle n_j n_j\rangle - \langle n_j\rangle^2 = \rho_j^c$.

The Hamiltonian in eq. (13) is invariant, up to a change in the chemical potential, under a particle–hole transformation, where the hole operators are the Hermitian conjugates of the boson operators, and the hole density

$$\rho_j^h = 1 - \rho_j. \tag{21}$$

Hence the condensate number density = $\rho_j^s = \rho_j(1-\rho_j) = \rho_j\rho_j^h$, showing that both particles and holes play equally important roles in determining the condensate behaviour. As we shall see, the particle–hole imbalance variable $\Delta_j = (1-2\rho_j) = (\rho_j^h - \rho_j)$ plays a key role in the dynamical evolution of the system.

5.3 *Order parameter equation for HCB condensate*

Equation (17) for S_j^+ leads to the following nonlinear differential difference equation for its spin-coherent state expectation value η_j:

$$i\hbar\frac{\partial\eta_j}{d\tau} = \left[\frac{(t-V)d}{2} - \mu\right]\eta_j - \frac{t}{2}(1-2\rho_j)\sum_a \eta_{j+a} + \frac{V}{2}\eta_j\sum_a(1-2\rho_{j+a}). \tag{22}$$

The continuum approximation of the discrete equation (22) is useful when the order parameter is a smoothly varying function with a length scale greater than the lattice spacing a. In the limit where the number of particles N and the number of lattice sites L tend to infinity, with the filling factor N/L fixed, the system is described by the condensate order parameter $\eta(\mathbf{r},\tau)$

$$\eta(\mathbf{r},\tau) = \sqrt{\rho(1-\rho)}\,\exp(i\phi). \tag{23}$$

On using the appropriate Taylor expansions of $\eta_{j\pm a}$ and $\rho_{j\pm a}$ in eq. (22), we obtain

$$i\hbar\frac{\partial\eta}{\mathrm{d}\tau} = -\frac{ta^2}{2}(1-2\rho)\nabla^2\eta - Va^2\,\nabla^2\rho\eta + 2(t-V)\mathrm{d}\rho\eta - \mu\eta. \tag{24}$$

By substituting eq. (23) in eq. (24), and equating its imaginary and real parts respectively, we obtain the following coupled nonlinear partial differential equations for ρ and ϕ:

$$\hbar\frac{\partial\rho}{\mathrm{d}\tau} = -ta^2\nabla\cdot\,[\rho(1-\rho)\,\nabla\phi] \tag{25}$$

and

$$\hbar\frac{\partial\phi}{\mathrm{d}\tau} = \frac{t\,(1-2\rho)a^2}{4{\rho^s}^2}\left(\rho^s\,\nabla^2\rho^s - \frac{1}{2}(\nabla\rho^s)^2 - 2{\rho^s}^2(\nabla\phi)^2\right) + Va^2\nabla^2\rho - 2(t-V)\mathrm{d}\rho + \mu, \tag{26}$$

where $\rho^s = \rho\,(1-\rho)$ from eq. (19). Equation (25) is the continuity equation for the HCB density ρ, with the corresponding current given by $\mathbf{J} = \frac{\hbar}{m}[\rho(1-\rho)]\,\nabla\phi$.

6. Linear and nonlinear excitations (solitons) in the HCB condensate

6.1 *Linear excitations of HCB condensate*

Using an analysis similar to that used in §3.1 for the GPE, the spectrum associated with the small amplitude modes of eq. (24) can be shown to be similar to that of the GPE. We shall therefore name (24) as HGPE, the letter H standing for 'hard-core'.

The corresponding (Bogoliubov-like) sound velocity for the HGPE for unidirectional propagation is

$$c_s^2 = 2t\,(t-V)\rho_0^s\;a^2/\hbar^2 = 2\rho_0^s\,(t-V)/m. \tag{27}$$

(Compare this with eq. (7).)

Since $t > 0$, we must have $(t-V) > 0$ for c_s to be real and nonzero.

6.2 *Nonlinear excitations (solitons) in the HCB condensate*

We now investigate if the HGPE (24) can support unidirectional soliton propagation in the x-direction. It turns out to be more convenient to work in terms of the variable θ instead of ρ. Hence we substitute $\rho = \sin^2\frac{\theta}{2}$ and $\rho^s = \rho(1-\rho) = \frac{1}{4}\sin^2\theta$ in eqs (25) and (26) to yield the following coupled nonlinear partial differential equations for θ and ϕ:

$$\hbar\sin\theta\theta_\tau = -\frac{ta^2}{2}[\phi_x\sin^2\theta]_x \tag{28}$$

$$\hbar\sin\theta\phi_\tau = [\mu-(t-V)]\sin\theta + (t-V)\sin\theta\cos\theta + \frac{ta^2}{2}\theta_{xx} - (t-V)\frac{a^2}{2}\left[\theta_{xx}\sin^2\theta + \sin\theta\cos\theta(\theta_x)^2\right] - \frac{ta^2}{2}\cos\theta\sin\theta\phi_x^2. \tag{29}$$

In the above, the subscripts τ and x denote partial derivatives.

In terms of ρ, eq. (28) becomes

$$\hbar\rho_\tau = -ta^2[\rho(1-\rho)\,\phi_x]_x. \tag{30}$$

We look for unidirectional travelling wave solutions of eqs (29) and (30) of the form $\phi = \omega\tau + \phi(z)$ and $\rho = \rho(z)$, where $z = (x - v\tau)/a$, where v is the velocity of the wave.

With the boundary conditions $\rho \to \rho_0$ and $\phi_z \to 0$ as $|z| \to \infty$, eq. (30) can be integrated to give

$$\phi_z = U(\rho - \rho_0)/\rho(1-\rho) = 4U\left(\sin^2\frac{\theta}{2} - \rho_0\right)/\sin^2\theta, \tag{31}$$

where $U = \hbar v/at$.

Using $\phi_\tau = \omega - (v/a)\phi_z$ in eq. (29) and substituting for ϕ_z from eq. (31), we find that multiplying both sides of the resulting equation by θ_z enables us to integrate it, with an integration constant C_2. Writing this equation in terms of ρ yields the nonlinear differential equation

$$\begin{aligned}\frac{1}{4}\rho_z^2\left[1 - 4E_2\rho(1-\rho)\right] = {} & U^2\left[-\rho_0^2 + (2\rho_0 - 1)\rho^2\right] + \rho(1-\rho) \\ & \times\left[(E_1 - E_2) - C_2 - 2\rho(E_1 - E_2\rho)\right],\end{aligned} \tag{32}$$

where

$$E_1 = (\mu - \hbar\omega)/t \tag{33}$$

and

$$E_2 = (t - V)/t. \tag{34}$$

Since we are interested in soliton solutions of eq. (32) that are localized, we use boundary conditions $\rho \to \rho_0$ and $\rho_z \to 0$ as $|z| \to \infty$, to determine C_2:

$$C_2 = -2\rho_0 U^2 + (E_1 - E_2) - 2\rho_0(E_1 - E_2\rho_0). \tag{35}$$

Substituting for C_2 from eq. (35) in eq. (32), we look for solutions of the form $\rho(z) = \rho_0 + f(z)$, where $f(z)$ denotes the density fluctuation above the background density ρ_0. This leads to the nonlinear differential equation

$$\frac{1}{4}\left(\frac{\mathrm{d}f}{\mathrm{d}z}\right)^2 [1 - 4E_2(\rho_0 + f)(1 - \rho_0 - f)] = K_1 f + K_2 f^2 + K_3 f^3 + K_4 f^4, \tag{36}$$

where

$$\begin{aligned} K_1 &= 2\rho_0(1-\rho_0)[2E_2\rho_0 - E_1]; \\ K_2 &= \left[2E_1(2\rho_0 - 1) + 2E_2\rho_0(3 - 5\rho_0) - U^2\right]; \\ K_3 &= 2E_1 + 2E_2(1 - 4\rho_0); \\ K_4 &= -2E_2. \end{aligned} \tag{37}$$

Note that there is no constant term on the right-hand side of eq. (36), consistent with the boundary condition $f(z) \to 0$ and $\mathrm{d}f/\mathrm{d}z \to 0$ as $|z| \to \infty$, that corresponds to the boundary condition on $\rho(z)$ that was used earlier to find C_2.

It is difficult to find an exact analytical solution for the nonlinear differential equation (36). However, we note that it is a good approximation to neglect [19] the nonlinear terms involving $f(\mathrm{d}f/\mathrm{d}z)^2$ and $f^2(\mathrm{d}f/\mathrm{d}z)^2$ compared to the other terms in the differential equation. Then, for $K_1 = 0$, localized soliton solutions arise, as we shall show. Now, the condition $K_1 = 0$ implies

$$E_1 = 2E_2\rho_0. \tag{38}$$

On substituting eqs (33) and (34) in the above, we see that

$$\omega = (\mu - 2(t - V)\rho_0)/\hbar. \tag{39}$$

Thus the physical significance of $K_1 = 0$ is that it determines ω, the angular velocity of the phase ϕ, in terms of the physical parameters of the system.

For $K_1 = 0$, eq. (36) becomes

$$\frac{1}{4}\left(\frac{\mathrm{d}f}{\mathrm{d}z}\right)^2 \left[1 - 4E_2\rho_0^s\right] = K_2 f^2 + K_3 f^3 + K_4 f^4, \tag{40}$$

where ρ_0^s is the background condensate density given by

$$\rho_0^s = \rho_0(1 - \rho_0). \tag{41}$$

On using eq. (38), the expressions in (37) become

$$\begin{aligned} K_2 &= (\hbar/ta)^2 \left(c_\mathrm{s}^2 - v^2\right); \\ K_3 &= (\hbar/ta)^2 c_\mathrm{s}^2 (1 - 2\rho_0)/\rho_0^s; \\ K_4 &= -(\hbar/ta)^2 c_\mathrm{s}^2 /\rho_0^s. \end{aligned} \tag{42}$$

In the above, c_s is the velocity of sound in the HCB condensate (see eq. (27) in §(6.1)).

$$c_\mathrm{s}^2 = \frac{2t(t - V)}{\hbar^2}\rho_0^s a^2. \tag{43}$$

In (45), the expression $(ta/\hbar)$ with dimensions of velocity appears in all the K_is, $i = 2, 3, 4$. It therefore becomes convenient to define a dimensionless sound velocity $\bar{c}_\mathrm{s}$ as

$$\bar{c}_\mathrm{s} = c_\mathrm{s}/(ta/\hbar) = \sqrt{2\rho_0^s (t - V)/t}. \tag{44}$$

Using this, eq. (45) becomes

$$K_2 = \bar{c}_\mathrm{s}^2\gamma^2; \quad K_3 = \bar{c}_\mathrm{s}^2 (1 - 2\rho_0)/\rho_0^s; \quad K_4 = -\bar{c}_\mathrm{s}^2 /\rho_0^s, \tag{45}$$

where

$$\gamma^2 = \left[1 - \frac{v^2}{c_s^2}\right]^2 = [1 - \bar{v}^2]^2, \tag{46}$$

with $\bar{v} = v/c_\mathrm{s}$.

Further, on using eqs (34) and (44), we see that in eq. (40), $\left(1 - 4E_2\rho_0^s\right) = \left(1 - 2\bar{c}_\mathrm{s}^2\right)$. Defining $\bar{z} = 2z/\sqrt{\left(1 - 2\bar{c}_\mathrm{s}^2\right)}$, eq. (40) becomes

$$\frac{\mathrm{d}f}{\mathrm{d}\bar{z}} = \pm\, f(K_2 + K_3 f + K_4 f^2)^{1/2}. \tag{47}$$

Equation (47) has two possible soliton solutions [19]

$$f^{\pm}(z) = \frac{2K_2}{\pm\sqrt{K_3^2 - 4K_2K_4}\,\cosh 2\sqrt{K_2}\bar{z} - K_3}. \tag{48}$$

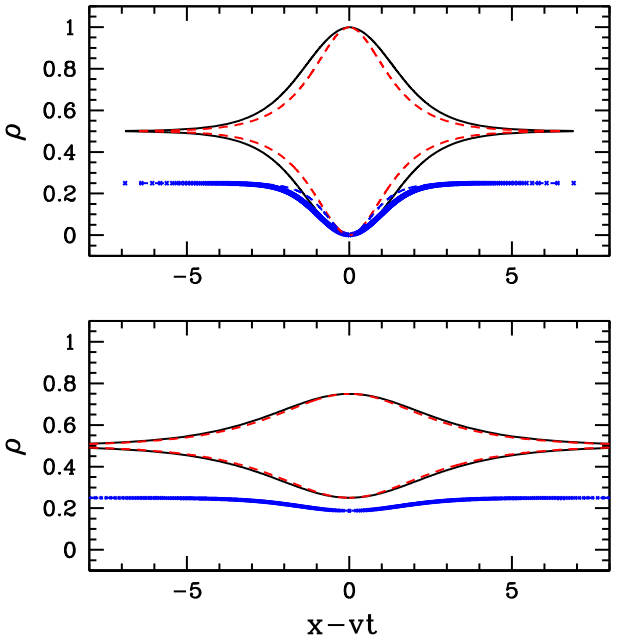

Figure 1. Comparison of numerical (solid line: black) and analytical (dashed line: red) solitary wave solutions, for $\rho_0 = 0.5$. The upper and lower panels correspond to $\bar{v} = 0, \gamma = 1$ and $\bar{v} = 0.87, \gamma = 0.5$, respectively. The plots with crosses (blue) show the corresponding condensate density ρ^s.

Substituting for $\bar{z}$ and K_2 (from (45)), the (dimensionless) width of the soliton Γ is found to be

$$\Gamma = \frac{\sqrt{1-2\bar{c}_s^2}}{4\bar{c}_s\gamma} = \frac{1}{2\gamma}\sqrt{\frac{\frac{1}{4}(1-2\rho_0)^2 + \frac{V}{t}\rho_0(1-\rho_0)}{2\left(1-\frac{V}{t}\right)\rho_0(1-\rho_0)}}. \tag{49}$$

Next, substituting the expressions for K_i, $i = 2, 3, 4$ from (45), the soliton solutions $f^{\pm}$ in (48) can be written in terms of dimensionless quantities as

$$f^{\pm}(z, \rho_0) = \frac{2\gamma^2\rho_0^s}{\pm\sqrt{(1-2\rho_0)^2 + 4\gamma^2\rho_0^s}\,\cosh(z/\Gamma) - (1-2\rho_0)}. \tag{50}$$

It must be mentioned that for $K_1 = 0$, we have also numerically integrated the full equation (36), i.e., without neglecting any terms on the left-hand side, to find $f(z)$, and compared it with our approximate analytical solution (48). We find close agreement between the two, showing that the approximation used by us (see paragraph above (38)) is indeed good. An example given in figure 1 with $\rho_0 = 1/2$ shows the case when the agreement is at its worst. Away from half-filling, we find that the numerical and analytical solutions are indistinguishable.

6.3 *Particle–hole symmetry in the soliton solutions*

Using eq. (21), we see that

$$(1-2\rho_0) = (\rho_0^h - \rho_0); \quad \rho_0^s = \rho_0\rho_0^h, \tag{51}$$

where ρ_0^h is the hole density in the background of the condensate. Using (51), the soliton solutions (50) can be written in the form

$$f^{\pm}(z) = \frac{2\gamma^2\rho_0\rho^h}{\pm\sqrt{(\rho_0^h-\rho_0)^2 + 4\gamma^2\rho_0\rho_0^h}\,\cosh(z/\Gamma) - (\rho_0^h-\rho_0)}, \tag{52}$$

where

$$\Gamma = \frac{1}{2\gamma}\sqrt{\frac{\frac{1}{4}\left(\rho_0^h-\rho_0\right)^2 + \frac{V}{t}\rho_0\rho_0^h}{2\left(1-\frac{V}{t}\right)\rho_0\rho_0^h}}. \tag{53}$$

It is readily seen from eqs (52) and (53) that if $f(z, \rho_0)$ is a solution, $f(z, \rho_0^h)$ is also a solution, with the relationship $f^{\pm}(z, \rho_0) = -f^{\mp}(z, \rho_0^h)$, which shows a certain particle–hole symmetry.

6.4 *Phase jump of the soliton*

From eq. (31), we write

$$\phi_z = (\hbar/ta)vf/(\rho_0+f)(1-\rho_0-f). \tag{54}$$

By substituting for the soliton solutions $f = f^{\pm}$ from eq. (50) and integrating both sides of eq. (54), a short calculation yields the phase jump $\Delta\phi$ as a function of $\bar{v}$ and ρ_0 as

$$\Delta\phi_{\pm} = 2\left(\sqrt{1-2c_s^2}\right)\cos^{-1}\frac{\bar{v}(1-2\rho_0)}{1-2\rho_0^s\bar{v}^2}, \tag{55}$$

where $\bar{v} = v/c_s$. Note that for small ρ_0^s (which implies values of ρ_0 near 0 or 1), the phase jump of the HCB soliton given above has the same form as that of the GPE soliton given in eq. (10).

7. Behaviour of the HCB solitons: Emergence of persistent solitons for $\rho_0 \neq 1/2$

As pointed out in §6.1, the solutions (50) are valid provided $(t - V) > 0$. Note that for $(t - V) < 0$, the sound velocity c_s becomes imaginary. As seen from the solution $f^{\pm}$ in eq. (50), the particle–hole imbalance $(\rho_0^h - \rho_0) = (1 - 2\rho_0)$ in the background is a key factor in determining the characteristics of the solitons.

(i) $\rho_0 = 1/2$
As seen from eq. (50) and also in figure 1, when the number of particles is equal to the number of holes, i.e., $\rho_0 = 1/2$ or half-filling case, the two solutions for the particle density $\rho^{\pm}(z) = \rho_0 + f^{\pm}$ are antidark and dark solitons, respectively, which are mirror images of each other, as seen in figure 1. As already mentioned, antidark

solitons [11] are just bright solitons on a pedestal, corresponding to $\rho_0 \neq 0$. The corresponding condensate density profiles $\rho^s(z)$ for the two solitons are identical at half-filling, resulting in a single soliton for the condensate. A short calculation shows that for $\rho_0 = 1/2$, the condensate density profile for the HCB soliton has the same functional form as that of the GPE dark soliton given in eq. (9). It flattens out at the sound velocity.

However for $\rho_0 = 1/2$, the phase jump of the HCB condensate is independent of v and is given by $\Delta\phi^{\pm} = \sqrt{1 - 2\bar{c}_s^2}\,\pi$, as seen from eq. (55). Thus at half-filling, the behaviour of the phase jump of the HCB soliton is different from that of the GPE dark soliton given in eq. (10), which is dependent on v in general.

For $\rho_0 \neq 1/2$, the particle density solitons are not mirror images of each other, as seen in figure 2a. We consider their behaviour below.

(ii) $0 < \rho_0 < 1/2$

When the number of particles differs from the number of holes, and $0 < \rho_0 < 1/2$, so that $(1 - 2\rho_0) > 0$, the condensate soliton corresponding to the solution f^- is gray even at $v = 0$. It grays further as v increases, and flattens out at the sound velocity. i.e., for $v \to c_s$,

$$\rho^- \ (0 < \rho_0 < 1/2) \ \rightarrow \ \rho_0. \tag{56}$$

However, the condensate soliton corresponding to the solution f^+ brightens the condensate profile, as shown in figure 2. As v increases, the spatial extent of the disturbance above the background increases, and the solitary wave $\rho^s(z)$ becomes

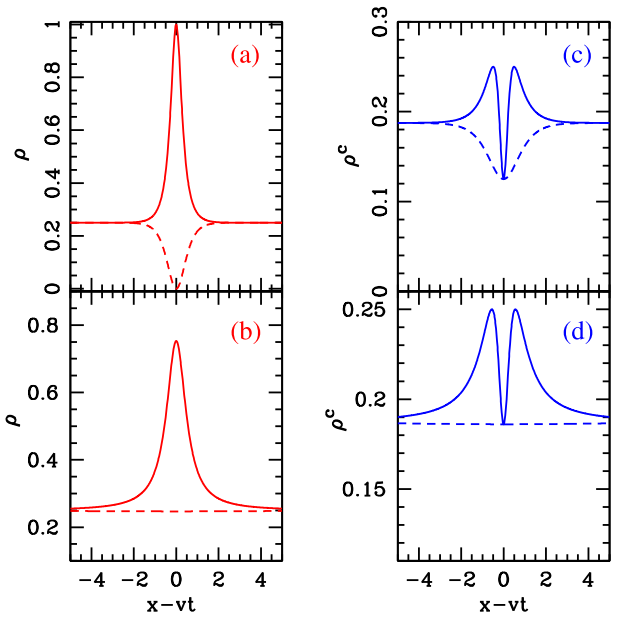

Figure 2. Solitary wave for $\rho_0 = 0.25$ for total particle density (**a**),(**b**) and condensate density (**c**),(**d**): $\bar{v} = 0$ (**a**),(**c**) and $\bar{v} = 1$ (**b**),(**d**). Solid (dotted) plots correspond to f^+ (f^-) solitons.

completely bright at the speed of sound. More important, this bright soliton (on a pedestal) does not flatten out but persists even at the sound velocity. The survival or persistence of the soliton of this sector is evident from the limiting functional form of f^+ as $v \to c_s$. We find that in this limit.

$$\rho^+ \ (0 < \rho_0 < 1/2) \ \to \ \rho_0 + \ \frac{1 - 2\rho_0}{1 + (z^2/\alpha^2)}, \tag{57}$$

where

$$\alpha^2 = \frac{(1-2\rho_0)^2}{\rho_0^s} \frac{\bar{c}_s^2}{1 - 2\bar{c}_s^2} = \frac{(1-2\rho_0)(1 - V/t)}{\left(\frac{1}{2} - \rho_0\right)^2 + (V/t)\rho_0(1-\rho_0)}. \tag{58}$$

(iii) $1/2 < \rho_0 < 1$

Here, since $(1 - 2\rho_0) < 0$, f^+ and f^- exchange roles that they had for $0 < \rho_0 < 1/2$. Therefore, as seen from the discussion of that case, here it is the dark (or rather, gray) soliton that persists even at the velocity of sound.

$$\rho^- \ (1/2 < \rho_0 < 1) \ \to \ \rho_0 - \ \frac{2\rho_0 - 1}{1 + (z^2/\alpha^2)}. \tag{59}$$

This is to be contrasted with the GPE dark soliton which flattens out at that velocity. On the other hand, the antidark soliton flattens out as $v \to c_s$.

$$\rho^+(1/2 < \rho_0 < 1) \to \rho_0. \tag{60}$$

Phase jump of the persistent soliton

The phase jump of the persistent solitons discussed in (ii) and (iii) can be calculated to yield

$$\Delta\phi_P(v \to c_s) = 2\pi\sqrt{1 - 2\bar{c}_s^2} \tag{61}$$

while

$$\Delta\phi_P(v \to 0) = \pi\sqrt{1 - 2\bar{c}_s^2}. \tag{62}$$

Before closing this section, we remark that even when $\rho_0 \to 0$, when the antidark solitons of the HCB become bright, their behaviour is quite distinct from the behaviour of the bright solitons of the attractive GPE discussed in §4.2. First, for the HCB case, both the amplitude and phase of the bright soliton travel with the same velocity, unlike the GPE bright soliton where they have different velocities. Secondly, there is no phase jump across the centre of the GPE bright soliton, contrary to the HCB case. Finally, for the attractive GPE soliton, there is no limiting velocity like the speed of sound, whereas in the HCB case, even the persistent soliton becomes a periodic wave form above the speed of sound, since γ becomes imaginary.

8. Energy–momentum dispersion relation of HCB solitons

In this section, we compute the energy–momentum dispersion relation for the dark and antidark solitons of the HCB condensate. This is obtained by first integrating the equation

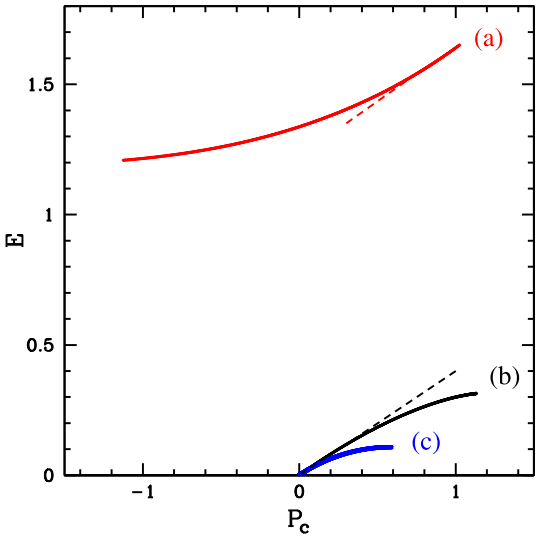

Figure 3. Energy vs canonical momentum for $\rho_0 = 0.25$. Curves (a) and (b) correspond to the persistent soliton and the gray soliton, respectively. Curve (c) gives the corresponding dispersion for the GPE soliton with $\rho = \rho_0^s$. The dashed tangents on the two curves demonstrate linear dispersion with identical slopes.

$\mathrm{d}E/\mathrm{d}P_\mathrm{c} = v$ [3] to obtain the canonical momentum P_c, where E is the energy, and then plotting E vs. P_c. As an example, we consider $\rho_0 = 0.25$. The three plots in figure 3 show the dispersion relations for the f^+ and f^- solitons [20], and the corresponding GPE soliton. Each plot shows linear dispersion at one end of the spectrum (at the momentum corresponding to $v = c_\mathrm{s}$), and saturation at the other end (at the momentum corresponding to $v = 0$). The gray soliton has a linear dispersion near $E = 0$, $P_\mathrm{c} = 0$, with the slope given by the speed of sound c_s, and it saturates to zero slope near the maximum value of the momentum. (The GPE soliton, with $\rho = \rho_0^s$, has a similar behaviour). The persistent soliton exhibits linear dispersion with the same slope c_s near the maximum value of the momentum. Comparing this with the exact bosonic low-lying excitation spectrum for the HCB gas in one-dimension discussed by Lieb [13], we note that both soliton branches with bounded momentum intervals, mimic the main characteristics of his type-II excitation spectrum, being linear at one end and saturating at the other.

9. Summary

Exploiting the fact that the Hamiltonian of a Bose–Hubbard lattice model with hard-core bosons and nearest-neighbour interactions maps to an anisotropic Heisenberg spin-1/2 Hamiltonian, we use spin-coherent states to describe the HCB condensate order parameter. We find that particles and holes play equal roles in the description of this condensate. Going over to a continuum description, we derive the nonlinear partial differential equation satisfied by the complex order parameter for the HCB condensate. Looking for unidirectional travelling wave solutions for density ρ, we find two types of solitons, the dark and

the antidark solitons, for the same background density ρ_0. Since the dark soliton is a wave that represents the absence of particles, while the antidark soliton is a wave that carries particles, the existence of these two solitons can be attributed to the presence of two distinct types of carriers, namely, particles and holes, in the HCB model.

For the half-filling case $\rho_0 = 1/2$, both the dark and antidark solitons for the density lead to the same dark soliton for the condensate density, which flattens out when its velocity approaches the sound velocity, like the GPE soliton. But its phase behaviour is different from that of the GPE soliton.

More interestingly, for $\rho_0 < 1/2$, the antidark soliton persists even at the speed of sound, while the dark soliton flattens out at that speed, like the GPE dark soliton. This brightening and persistence of a soliton in the condensate density are novel features, since repulsive bosons are expected to support only a dark soliton. In contrast, for $\rho_0 > 1/2$, the antidark soliton flattens out at the speed of sound, while the dark soliton persists even at that speed. This dark soliton which has a nonvanishing amplitude all the way up to the speed of sound is yet another novel feature of the HCB system, since all previously known solitons die down at sonic speeds. Our persistent soliton has also been named 'immortal soliton' and 'everlasting quantum wave' [21].

Our analytic solution (50) is useful in giving the functional forms of the initial profiles at $t = 0$ that can be used for numerical computations on the lattice. We hope our results on persistent solitons in the HCB condensate will provide a motivation for the experimental generation of these nonlinear excitations using phase engineering methods [5].

Finally, we remark that although we have used the term 'soliton' for our dark and antidark solutions $f^{\pm}$, they have been obtained only as solitary wave solutions. But the similarity found in §8 between the energy–momentum dispersion for the solitary wave solutions of the order parameter, which is the coherent state expectation value of the HCB annihilation operator, and Lieb's exact quantum excitation spectrum for the HCB system, suggests that our unidirectional solitary waves are perhaps strict solitons. In other words, since the one-dimensional quantum HCB system is exactly solvable, the associated one-dimensional classical HGPE (24) satisfied by its order parameter may also be a completely integrable equation. If so, it will possess a Lax pair, an infinite number of conserved quantities, multisoliton solutions, etc. [1]. In fact, detailed numerical studies [22] have recently confirmed that the dark and antidark solitary waves that we have found for the HCB condensate are indeed solitons, as they remain intact under collision.

Acknowledgements

RB thanks the Department of Science and Technology, India, for financial support.

References

[1] M J Ablowitz and H Segur, *Solitons and the inverse scattering transform* (SIAM, Philadelphia, 1981)
[2] T Dauxois and M Peyard, *Physics of solitons* (Cambridge University Press, Cambridge, 2006)
[3] See, for instance, L Pitaevskii and S Stringari, *Bose–Einstein condensation* (Oxford University Press, Oxford, 2003), and references therein
[4] S Burger *et al*, *Phys. Rev. Lett.* **83**, 5198 (1999)

[5] J Denschlag *et al*, *Science* **287**, 97 (2000)
[6] L Khaykovich *et al*, *Science* **292**, 1290 (2002)
[7] E Kolomeisky, T J Newman, J Straley and X Qi, *Phys. Rev. Lett*. **85**, 1146 (2000)
[8] G L Alfimov *et al*, *Phys Rev*. **A75**, 023624 (2007)
[9] B B Baizakov *et al*, *J. Phys. B: At. Mol. Opt. Phys.* **42**, 175302 (2009)
[10] Radha Balakrishnan, Indubala I Satija and C W Clark, *Phys. Rev. Lett*. **103**, 230403 (2009)
[11] Y S Kivshar and V V Afanasjev, *Phys. Rev*. **A44**, R1446 (1991)
[12] E H Lieb, R Seiringer and J Yngvason, *Phys. Rev. Lett*. **91**, 150401 (2003)
[13] E H Lieb, *Phys. Rev*. **130**, 1616 (1963)
[14] See, for example, S Sachdev, *Quantum phase transitions* (Cambridge University Press, Cambridge, 1999)
[15] T Matsubara and H Matsuda, *Prog. Theor. Phys*. **16**, 569 (1956)
[16] Radha Balakrishnan, R Sridhar and R Vasudevan, *Phys. Rev*. **B39**, 174 (1989)
[17] J M Radcliffe, *J. Phys.* **A4**, 313 (1971)
[18] J S Langer, *Phys. Rev*. **167**, 183 (1968)
[19] Radha Balakrishnan, *Phys. Rev*. **B42**, 6153 (1990). Our present analysis differs slightly from that given in this reference.
[20] The integration is done using the boundary condition $P_c^- = 0$ when $v = v_s$ for the f^- soliton. For the f^+ soliton, we use the condition $P_c^+(v = 0) = -P_c^-(v = 0)$, because the twin solitons have equal and opposite phase jumps at $v = 0$
[21] See for instance, www.sciencedaily.com/releases/2009/12/091217102256.htm; www.physorg.com/news180207149.html
[22] William P Reinhardt, Indubala I Satija, Bryce Robbins and Charles W Clark, arXiv:1102. 4042 [quant-ph]